Comparison of Control Strategies for AC/DC Converter for a Wind Energy System with Permanent Magnet Synchronous Generator

Gallo Tibanquiza, Alberto Enrique y Taco Chuquitarco, Darwin Rodrigo

Departamento de Eléctrica, Electrónica y Telecomunicaciones

Carrera de Ingeniería en Electrónica e Instrumentación

Artículo académico, previo a la obtención del título de Ingeniera en Electrónica e Instrumentación

Msc. Velasco Sánchez, Paola Maritza, Tutora

Ph.D Llanos Proaño, Jacqueline del Rosario Co-Tutora

7 de diciembre del 2023

Latacunga

Comparison of Control Strategies for AC/DC Converter for a Wind Energy System with Permanent Magnet Synchronous Generator

Darwin Taco
Universidad de las Fuerzas Armadas ESPE
Sangolquí-Ecuador
drtaco1@espe.edu.ec

Enrique Gallo
Universidad de las Fuerzas Armadas ESPE
Sangolquí-Ecuador
aegallo@espe.edu.ec

Paola Velasco
Universidad de las Fuerzas Armadas ESPE
Sangolquí-Ecuador
pmvelasco1@espe.edu.ec

Jacqueline Llanos
Universidad de las Fuerzas Armadas ESPE
Sangolquí-Ecuador
jdllanos1@espe.edu.ec

Jorge Vega
Universidad de Antofagasta
Antofagasta-Chile
jorge.vega@uantof.cl

***Abstract*—Wind energy contributes to diversifying the energy matrix. These systems can be adapted to various scales, from industrial wind farms to smaller residential systems, makingaccessible and versatile. Furthermore, wind systems promotes environmental preservation by reducing dependence on nonrenewable energy sources like fossil fuels, significantly contributing to climate change mitigation. The challenge posed by wind energy lies in controlling it against disturbances with high variability, such as wind speed. To address this challenge, advanced control systems must be implemented to optimize the performance of wind turbines and minimize the adverse effects of varying wind conditions. This work presents the design and implementation of two control strategies for the AC/DC converter of a wind system with a PMSG generator. First a traditional PI controller is used, followed by a PI+Fuzzy-PI controller. The aim is to analyze and compare the dynamic performance of both control techniques. The results show that the PI+Zuzzy-PI controller has a better dynamic performance than PI controller. The overshoot and settling time can be reduced in the former. Therefore, the effectiveness of PI+Fuzzy – PI controller is evaluated and demonstraed.**

Keywords—wind energy system, fuzzy control, AC/DC converter.

I. INTRODUCTION

The increase in global demand for electric energy has driven the search for new sustainable and efficient generation sources. This aims to minimize the environmental impact of the generation of traditional energy sources[1]. In the last decade, there has been a significant increase in the production of electric energy from wind turbines. Wind energy is a renewable energy source widely accepted in various countries due to its low environmental impact and ability to reduce implementation costs [2], [3].

Wind energy generation presents significant challenges due to the variability of the wind speed. This fluctuation makes it difficult to control the variables associated with wind energy generation [4]. Therefore, the electricity produced by wind turbines cannot be directly connected to a load [5]. Control systems are applied to power electronics to address the challenge of variability in this renewable energy source [6].

Among the different wind power technologies that operate at variable wind speeds, technologies that use permanent magnet synchronous generators (PMSG) require less maintenance and are connected to the grid through power electronics. Also, it requires low maintenance [7], [8]. The converter enables the maximization of natural resources. The control systems are commonly implemented in dq reference frame [5]. This allows for controlling active and reactive power separately. Thus, the maximum power point tracker (MPPT) can be achieved. The controllers typically implemented in dq are proportional and integral (PI) controllers. It has been shown that the PI control may cause good dynamic performance if the controller is adequately tuned [9] [10]. However, systems with high – levels of wind power plants with PMSG may experience poor dynamic performance due to new interactions. For example, in [11] [12] , poor dynamic performance has been observed when the injected power is high, and the point where the wind power is connected has a low level of the short circuit [13].

Given the context above, novel control systems have been proposed for wind power plants with PMSG. This has been possible due to the advance in power electronic technologies. Fuzzy control has emerged as a promising solution among the various proposals. This approach uses fuzzy sets and linguistic rules to make decisions based on uncertain or imprecise inputs. Notably, in PMSG, it may optimize its performance based on varying wind conditions [14], [15].

This research compares control algorithms applied to the AC/DC converter for transforming wind energy. A traditional PI control strategy in dq coordinates is tested and compared with an advanced fuzzy logic-based controller. The performance of the controllers is validated under various wind speed scenarios through real-time simulator Typhoon HIL. The experimental tests are programmed on a DSP. In these simulators, the actual plant's emulation includes the wind turbine, the AC/DC converter, the designed filters, and the loads [16].

The main contributions of this work are: i) comparing and identifying the best control algorithm for the AC/DC converter in wind power generation, ii) showcasing experimental results implemented on a DSP when subjected to various disturbances, in this case, different wind speeds. iii) Allowing good performance against various disturbances.

II. WIND SYSTEM MODEL

The Wind Energy Conversion System (WECS) shown in Figure 1 is composed of a PMSG generator with

979-8-3503-2504-1/23/$31.00 ©2023 IEEE

characteristics listed in Table II, and the converter is controlled using PWM. Furthermore, it consists of an RL filter designed to eliminate harmonic distortion in the currents and limit abrupt current changes. It also includes a constant voltage source that emulates a fixed local load. This is placed to validate the performance of the AC/DC converter controller, assuming that control in v_{dc} is constant. This is done because, in this stage, the aim is to identify the best control applied to the AC/DC converter. [17].

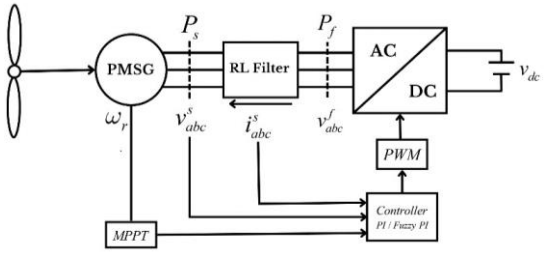

Fig. 1. Diagram of an AC/DC Wind Energy Conversion System (WECS) based on a Permanent Magnet Synchronous Generator (PMSG).

A. PMSG Model

The Park model is a common model of the PMSG generator in the d-q reference frame. The stator voltages v^s_{abc} in the d-q reference frame (v^s_d and v^s_q) are defined by (1) and (2), respectively. Where R_s is the stator winding resistance, ω_e represents the angular frequency of the rotating shaft associated with the d-q axes, i_{sd} and i_{sq} are the stator current in the d-q reference frame, and ψ_{sd} and ψ_{sq} are the stator fluxes in the d-q reference frame generated by the machine due to its magnets, defined by (3) and (4). L_s is the leakage inductance of the PMSG. The terms ψ_{fd} and ψ_{fq} correspond to the constant flux of the machine itself. [18].

$$v^s_d = -R_s i_{sd} - \frac{d\psi_{sd}}{dt} - \omega_e \psi_{sq} \tag{1}$$

$$v^s_q = -R_s i_{sd} - \frac{d\psi_{sq}}{dt} + \omega_e \psi_{sd} \tag{2}$$

$$\psi_{sd} = L_s i_{sd} + \psi_{fd} \tag{3}$$

$$\psi_{sq} = L_s i_{sq} + \psi_{fq} \tag{4}$$

Surface-mounted PMSGs have a uniform air gap, so the inductances in the d and q axes are identical. By substituting (3) and (4) into (2) and (1), we obtain (5) and (6):

$$v^s_d = -R_s i_{sd} - \frac{d\psi_{sd}}{dt} - \omega_e L_s i_{sq} - \omega_e \psi_{fq} \tag{5}$$

$$v^s_d = -R_s i_{sd} - \frac{d\psi_{sd}}{dt} - \omega_e L_s i_{sq} - \omega_e \psi_{fq} \tag{6}$$

In [19], it is mentioned that PMSG generators (Permanent Magnet Synchronous Generators with surface-mounted magnets) have a uniform air gap; hence, the inductances in the d-q axis are identical. If a the fluxes are considered constants , the derivatives of the fluxes $\frac{d\psi_{sd}}{dt} = 0$ and $\frac{d\psi_{sq}}{dt} = 0$ Further, assuming $R_s \approx 0\ \Omega$ and $L_s \approx 0H$, the PMSG model yields to (7) and (8):

$$v^s_d = -\omega_e \psi_{fq} \tag{7}$$

$$v^s_q = \omega_e \psi_{fd} \tag{8}$$

B. Maximum Power Point Tracking (MPPT)

The concept of MPPT applies in the context of wind turbines, where it involves the constant search for the relationship between the machine's rotational speed and the active power defined by (9), where P_s is the generated active power, ω_r is the mechanical rotational speed of the generator in rpm, K_{opt} is a constant involving blade pitch and other factors. This contributes to wind optimization to maximize generated power [20]. The optimization is achieved through the precise adjustment of the orientation and rotational speed of the turbine blades, allowing for the maximum utilization of the kinetic energy contained in the wind. [21].

$$P_s = K_{opt} \omega_r^3 \tag{9}$$

III. Design of the AC/DC Converter Controllers

In this section, two control strategies are designed. The first is a PI controller, and the second is a Fuzzy control. The latter is based on fuzzy logic, which includes fuzzy sets and linguistic rules to make decisions in situations with uncertainty. These control strategies aim to ensure good dynamic performance and stability of PMSG in grid connection mode. Further, the control strategies are designed considering various operating conditions due to wind speed.

A. PI Controller Design

Figure 2 displays the control diagrams utilized for the system described in equations (5) and (6). Two current control loops are defined. The error between the current at the output of the machine i^s_d and the reference current of the machine i^{s*}_d is corrected by the controller. The reference current i^{s*}_d is obtained from the MPPT to achieve the maximum active power of the machine. Similarly, the error between i^{s*}_q and i^s_q is corrected by a PI controller. The desired current is set to 0, which allows achieving a power factor of 1 on the generator side.

Figure 2b shows the designed PI control, for which the process model $H(s)$ is required, to which a controller characterized by its transfer function $PI(s)$ is applied. The closed-loop transfer function in equation (10) relates the controller's input to the process output. Where k_p is the proportional gain and k_i is the integral gain of the PI controller, R and L are the resistance and inductance of the filter.

$$M(s)=\frac{k_p}{sL}\left(\frac{s+\frac{k_i}{k_p}}{s+\frac{R}{L}}\right) \tag{10}$$

The pole is very close to the origin, so it cancels out by zero to obtain the gains k_i and k_p, and the equality from (10) as described in (11) yields the closed-loop transfer function (12) Where $\tau=\frac{L}{k_p}$ and $k_i=\frac{R}{\tau}$ [20].

$$\left(\frac{k_i}{k_p}=\frac{R}{L}\right) \tag{11}$$

$$G(s)=\frac{l(s)}{1+l(s)}=\frac{1}{\tau s+1} \tag{12}$$

To obtain the d-q components of feedback voltage after obtaining the control actions u_d and u_q, the cross-coupling terms should be used as described in (5) and (6). The inverse Park transform dq/abc is used to obtain the three-phase reference voltage v^*_{abc} with an angle theta θ. The voltages are then sent to a PWM block that modulates the signals to control the AC/DC converter.

a)

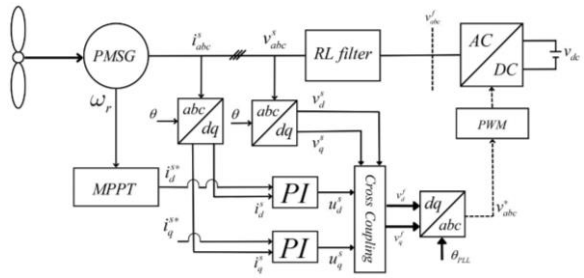

b)

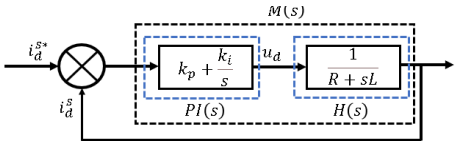

Fig. 2. Control PI. a) Architecture diagram of the PI control for the generator-side AC/DC converter. b) Algorithm diagram of the PI control

B. *Fuzzy Control Algorithm Design*

The architecture of the PI + Fuzzy PI control (See Fig. 3) incorporates two stages: a PI controller with gains (k_p and k_i) in the first stage and the second stage corresponding to the fuzzy PI control algorithm, which requires gains (k_e and k_{pe}).

The fuzzy PI uses two input variables: error and the integral of error, each multiplied by their respective gains, which are designed to have a range of [-30, 30], similar to the fuzzy output. The inputs are defined using seven fuzzy sets, employing triangular membership functions, except for the extremes where trapezoidal membership functions are used. The fuzzy sets are associated with the following linguistic variables: Negative Big (NB), Negative Medium (NM), Negative Small (NS), Zero (Z), Positive Small (PS), Positive Medium (PM), and Positive Big (PB). Figure 4 provides a visualization of these fuzzy sets representing both error and the integral of error [22].

For the output variable, nine fuzzy sets have been defined, evenly distributed within the range of [-30, +30], using triangular membership functions, as shown in Figure 5. These fuzzy sets are associated with the following linguistic variables: Very Negative Big (NBB), Negative Big (NB), Negative Medium (NM), Negative Small (NS), Zero (Z), Positive Small (PS), Positive Medium (PM), Positive Big (PB), and Very Positive Big (PBB). As presented in Table I, forty-nine control rules have been formulated using the IF-AND-THEN structure. Finally, the centroid technique is used as defuzzification [23].

As observed in Figure 3, the output of the fuzzy controller passes through an integrator stage and is simultaneously multiplied by the gain k_i, which serves as conditioning between the fuzzy control with an output range of [-30 to 30] and the overall control action, which corresponds to a standard voltage signal ranging from 0 to 1200 volts. This voltage signal is defined by v_{dc} and, in this case, emulates the load [24].

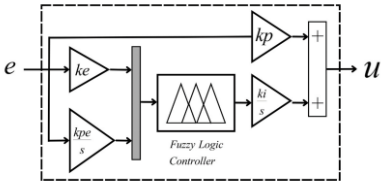

Fig. 3. Design of the PIFPI fuzzy logic control scheme.

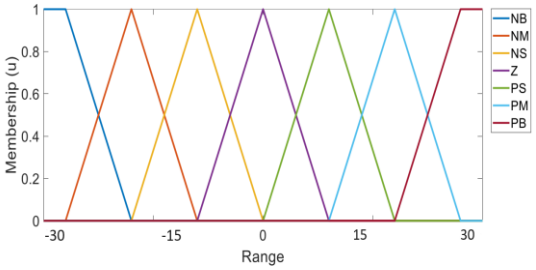

Fig. 4. Membership functions of the input variables.

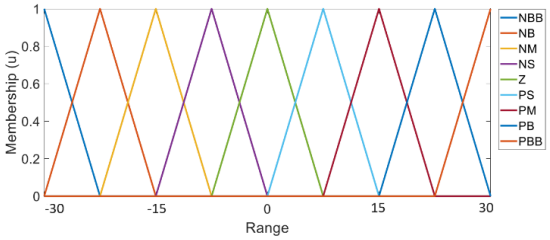

Fig. 5. Membership functions of the output variables.

TABLE I. FUZZY RULE BASE

e/ie	NB	NM	NS	Z	PS	PM	PG
NB	NBB	NBB	NBB	NB	NM	NS	Z
NM	NBB	NBB	NB	NM	NS	Z	PS
NS	NBB	NB	NM	NS	Z	PS	PM
Z	NB	NM	NS	Z	PS	PM	PB
PS	NM	NS	Z	PS	PM	PB	PBB

PM	NS	Z	PS	PM	PB	PBB	PBB
PB	Z	PS	PM	PB	PBB	PBB	PBB

Figure 6 shows the schematic control diagram of the generator side. It is important to clarify that both PI+Fuzzy PI current controllers use the same gains, and the input variables are the same, as described in section A. Likewise, the cross-coupling.

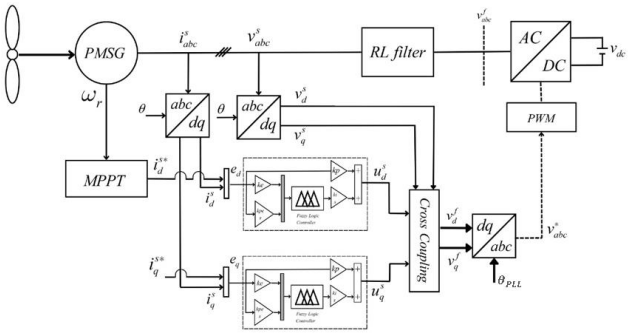

Fig. 6. Schematic of the PI fuzzy control strategy for the generator-side converter.

C. *Design of a Phase-Locked Loop (PLL)*

The design of a second-order PLL, where v^s_{abc}, which are converted to d-q, depend on the angle θ_{PLL}, with the purpose of ensuring that the voltage on the q-axis remains at zero, incorporates a PI controller, as shown in Figure 7. [11]. The PLL is used in the PI and fuzzy control to obtain the coordinate transformation.

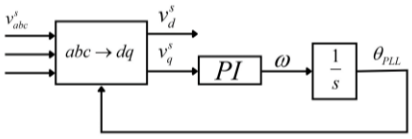

Fig. 7. Block diagram of the PLL.

IV. RESULTS

In this section, the effectiveness of the controllers designed in Section III is evaluated experimentally. The Typhoo HIL and DSP controller are used and applied to the wind generator that responds to the model presented in Section II. The controllers are implemented experimentally in the Typhoon HIL system, as shown in Figure 8a.

Figure 8a includes two sections. The first section consists of a PMSG generator, a filter, and the power electronics interface, the AC/DC converter. The second section corresponds to the control implemented in the Digital Signal Processor (DSP) TMS320F28335 from Texas Instruments, which sends PWM signals to the converter. Figure 8b shows the experimental setup topology.

a)

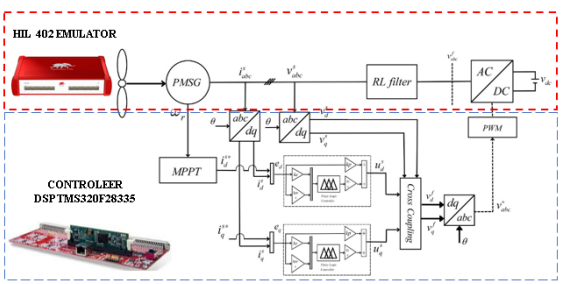

b)

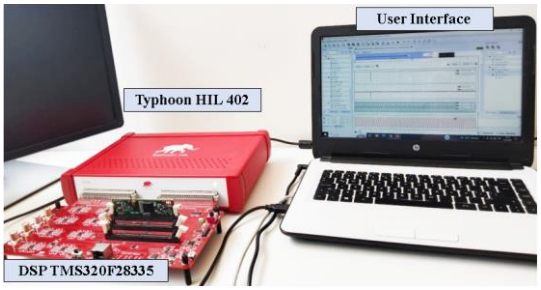

Fig. 8. Experimental implementation a) Implementation of the plant and control. b) Real experimental implementation.

One of the fundamental aspects in the implementation of control systems is the determination of specific parameters that characterize the system. The model parameters and controller gains are shown in Table II.

TABLE II. SYSTEM PARAMETERS AND CONTROLLER GAINS

Description	**Parameters**	**Values**
Nominal power	$P_{n,PMSG}$	$75kW$
Number of pole pairs	p	4
Resistor (Filter)	R	0.25Ω
Inductante (Filter)	L	$0.007H$
Machine Constant	k_{opt}	$0,0001778$
Permanent magnetic flux	ψ_{fq}	$1.7933Wb$
Nominal rotational speed	w_m	$750rpm$
Nominal DC voltage	V_{dc}	$1200V$
Current control PI	(k_p, k_i)	$(4.398, 157.079)$
Current control PI+Fuzzy PI	(k_e, k_{pe}, k_i, k_p)	$(0.066, 0.32, 1200, 12)$
PLL control	$(k_{p,PLL}, k_{i,PLL})$	$(125.66, 394784.176)$
Description	**Parameters**	**Values**
Nominal power	$P_{n,PMSG}$	$75kW$
Number of pole pairs	p	4
Resistor (Filter)	R	0.25Ω
Inductante (Filter)	L	$0.007H$
Machine Constant	k_{opt}	$0,0001778$
Permanent magnetic flux	ψ_{fq}	$1.7933Wb$
Nominal rotational speed	w_m	$750rpm$
Nominal DC voltage	V_{dc}	$1200V$
Current control PI	(k_p, k_i)	$(4.398, 157.079)$
Current control Fuzzy PI	(k_e, k_{pe}, k_i, k_p)	$(0.066, 0.32, 1200, 12)$
PLL control	$(k_{p,PLL}, k_{i,PLL})$	$(125.66, 394784.176)$

In order to evaluate the performance of the PI and Fuzzy-PI controllers, disturbances in wind speed are considered. The performance is presented in Figures 9 and 10. Figure 9 depicts the evolution of machine currents (i^S_d, i^S_q) when there is a speed change from $500rpm$ to $600rpm$ within one second, which is equivalent to a change in the reference current $i^{S*}_d = 85.2[A]$ representing the 80% change in nominal speed. The power factor is set to 1, which means that the machine is injecting active power. Also, the v_{dc} remains constant at $1200V$.

Both controllers can reach the desired current value in steady-state, as observed. However, it can be observed that there is a reduction in the oscillation of the stator current i_q^s with the PI+Fuzzy PI controller. The settling time is shorter and does not exhibit overshoot, whereas the traditional PI controller shows a slight overshoot (see Fig. 10).

The PI+Fuzzy PI controller exhibits a faster response to changes in reference currents and a small variation once the current stabilizes. While with the traditional PI controller, small oscillations can be observed due to PWM modulation and non-ideal characteristics of the converter. Table III presents the performance parameters of the two implemented controllers, showing better performance of the PI+Fuzzy PI controller when analyzing parameters in transient and steady-state.

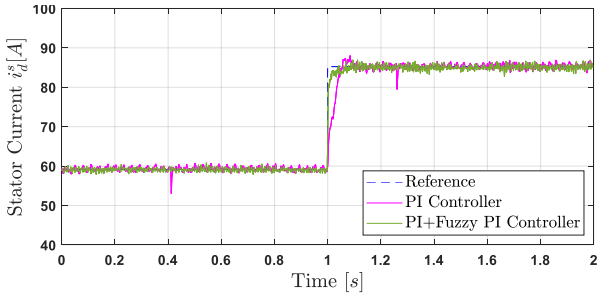

Fig. 9. Comparison of the controllers (PI, PI+Fuzzy PI) for the direct component of machine current i_d^s .

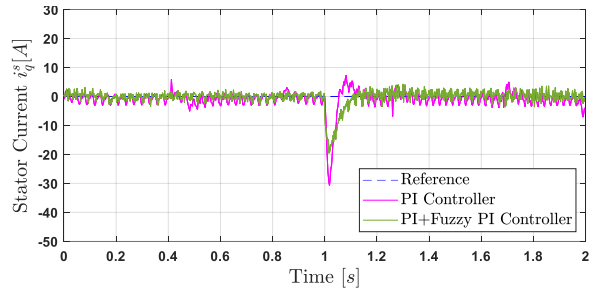

Fig. 10. Comparison of the controllers (PI, Fuzzy-PI) for the quadrature component of machine current i_q^s .

TABLE III. OPERATING PARAMETERS OF THE CONTROLLER IN DIRECT CURRENT VARIABLE

Parameters	PI	PI+Fuzzy PI
Overshoot	2.3%	0%
Settling time	0.116s	0.094s
Steady-state error	0.44A	0.1A

In Figure 11, the three-phase currents of the machine are shown. A speed change is made in 1 second. It is seen that the current increases to $85.2[A]$. This value is equivalent to the current in the d-coordinate, i_d^s. Additionally, the system control is adjusted to meet the control objective.

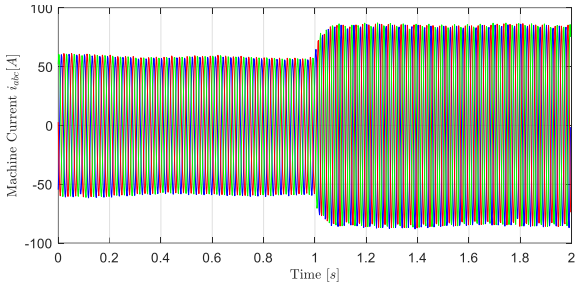

Fig. 11. Machine Current i_{abc}

Figure 12 shows the response of the PLL on the machine side. To evaluate the performance of the PLL, two speed changes were made. The first change was from $500rpm$ to $600rpm$ in $1.7s$, and the second change was from $600rpm$ to $650rpm$ in $3.33s$. En la Fig. 12 muestra la respuesta del PLL en el lado de la máquina. Para evaluar el rendimiento del PLL, se realizaron dos cambios de velocidad en la primera de $500rpm$ a $600rpm$ en el tiempo de $1.7s$ después el segundo cambio se realizó de $600rpm$ a $650rpm$ en $3.33s$. It can be observed that the PLL functions effectively in response to speed and angular frequency variations of the machine, achieving zero steady-state error.

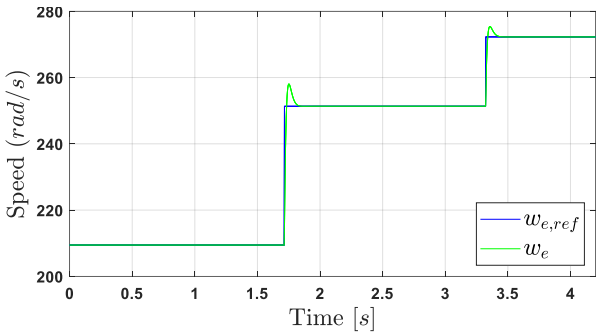

Fig. 12. PLL response on the machine side.

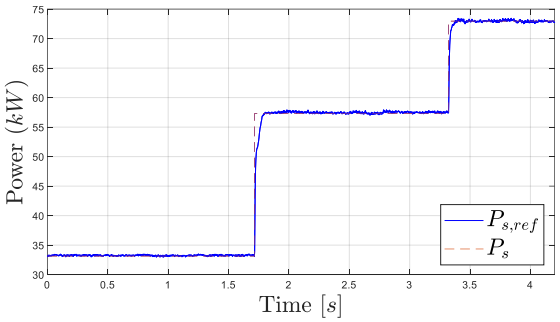

Fig. 13. The active power P_s of the wind generator system

In Figure 13, the active power response to wind disturbances can be observed, and it converges to the same value in steady-state with both implemented control techniques. These results indicate a constant active power output.

V. Conclusions

This work evaluates two control techniques, PI and PI+Fuzzy-PI, in a WECS-PMSG system through their experimental implementation in Typhoon HIL. The findings indicated that both controllers had zero steady-state error under various wind speed scenarios. However, the PI+Fuzzy-PI controller outperformed, showing a faster response with a

shorter settling time and less stator current oscillation than the PI controller. An important aspect was that the PI+Fuzzy-PI controller did not exhibit an overshoot in the direct current. These results highlight the effectiveness of the PI+Fuzzy-PI controller in the context of the WECS-PMSG system and its ability to improve system response and stability. Typhoon HIL allows for practical real-time emulation of wind energy systems and power electronics, saving costs by avoiding the need for expensive physical prototypes. It also facilitates detailed analysis and optimization of wind energy systems.

VI. Acknowledgments

This work was supported in part by the Universidad de las Fuerzas Armadas ESPE through the Project "Optimal energy management systems for hybrid generation systems", under Project 2023-pis-03.

References

[1] E. L. Valencia-Bautista, R. J. Angulo-Guerrero, J. M. Farfán-Bone, I. A. Arboleda-Cheres, C. J. Verá-Lozano, y T. J. Orobio-Arboleda, «Una revisión del suministro de energía renovable y las tecnologías de eficiencia energética A review of renewable energy supply and energy efficiency technologies», vol. 7, n.º 4, 2022.

[2] F. A. Cruz-Garcia *et al.*, «Estudio de factibilidad económica del Parque eólico "BII CUBI"», en *2017 IEEE 37th Central America and Panama Convention (CONCAPAN XXXVII)*, Managua: IEEE, nov. 2017, pp. 1-8. doi: 10.1109/CONCAPAN.2017.8278477.

[3] M. G. Molina y P. E. Mercado, «ESTRATEGIA DE CONTROL PARA MAXIMIZAR LA POTENCIA EXTRAÍDA DE AEROGENERADORES DE VELOCIDAD VARIABLE CONECTADOS A LA RED ELÉCTRICA».

[4] J. G. Slootweg, S. W. H. De Haan, H. Polinder, y W. L. Kling, «General model for representing variable speed wind turbines in power system dynamics simulations», *IEEE Trans. Power Syst.*, vol. 18, n.º 1, pp. 144-151, feb. 2003, doi: 10.1109/TPWRS.2002.807113.

[5] A. D. Hansen y G. Michalke, «Modelling and control of variable-speed multi-pole permanent magnet synchronous generator wind turbine», *Wind Energy*, vol. 11, n.º 5, pp. 537-554, sep. 2008, doi: 10.1002/we.278.

[6] Y. G. Landera, L. L. Viltre, G. Q. de Basterra, y D. L. León, «Revisión de controladores de corriente para condiciones LVRT en un sistema fotovoltaico: Review of current controllers for LVRT conditions in a grid-connected photovoltaic system», *Ing. Energética*, vol. 43, n.º 2, Art. n.º 2, jun. 2022.

[7] E. Santacana, T. Zucco, X. Feng, J. Pan, M. Mousavi, y L. Tang, «Energía para la eficiencia».

[8] J. A. Baroudi, V. Dinavahi, y A. M. Knight, «A review of power converter topologies for wind generators», *Renew. Energy*, vol. 32, n.º 14, pp. 2369-2385, nov. 2007, doi: 10.1016/j.renene.2006.12.002.

[9] A. Rolan, A. Luna, G. Vazquez, D. Aguilar, y G. Azevedo, «Modeling of a variable speed wind turbine with a Permanent Magnet Synchronous Generator», en *2009 IEEE International Symposium on Industrial Electronics*, Seoul, South Korea: IEEE, jul. 2009, pp. 734-739. doi: 10.1109/ISIE.2009.5218120.

[10] B. S. Theja, A. Rajasekhar, D. P. Kothari, y S. Das, «Design of PID controller based power system stabilizer using Modified Philip-Heffron's model: An artificial bee colony approach», en *2013 IEEE Symposium on Swarm Intelligence (SIS)*, Singapore,, Singapore: IEEE, abr. 2013, pp. 228-234. doi: 10.1109/SIS.2013.6615183.

[11] L. Fan, «Modeling Type-4 Wind in Weak Grids», *IEEE Trans. Sustain. Energy*, vol. 10, n.º 2, pp. 853-864, abr. 2019, doi: 10.1109/TSTE.2018.2849849.

[12] T. Xue, J. Lyu, H. Wang, y X. Cai, «A Complete Impedance Model of a PMSG-Based Wind Energy Conversion System and Its Effect On the Stability Analysis of MMC-HVDC Connected Offshore Wind Farms», *IEEE Trans. Energy Convers.*, vol. 36, n.º 4, pp. 3449-3461, dic. 2021, doi: 10.1109/TEC.2021.3074798.

[13] L. Fan y Z. Miao, «Wind in Weak Grids: 4 Hz or 30 Hz Oscillations?», *IEEE Trans. Power Syst.*, vol. 33, n.º 5, pp. 5803-5804, sep. 2018, doi: 10.1109/TPWRS.2018.2852947.

[14] M. Mansour, M. N. Mansouri, S. Bendoukha, y M. F. Mimouni, «A grid-connected variable-speed wind generator driving a fuzzy-controlled PMSG and associated to a flywheel energy storage system», *Electr. Power Syst. Res.*, vol. 180, p. 106137, mar. 2020, doi: 10.1016/j.epsr.2019.106137.

[15] L. Pan y X. Wang, «Variable pitch control on direct-driven PMSG for offshore wind turbine using Repetitive-TS fuzzy PID control», *Renew. Energy*, vol. 159, pp. 221-237, oct. 2020, doi: 10.1016/j.renene.2020.05.093.

[16] B. P. Ganthia, S. K. Barik, y B. Nayak, «Hardware in Loop (THIL 402) Validated Type-I Fuzzy Logic Control of Type-III Wind Turbine System under Transients», *J. Electr. Syst.*, vol. 17, n.º 1, pp. 28-51, 2021.

[17] R. Cardenas, R. Pena, M. Perez, J. Clare, G. Asher, y F. Vargas, «Vector Control of Front-End Converters for Variable-Speed Wind–Diesel Systems», *IEEE Trans. Ind. Electron.*, vol. 53, n.º 4, pp. 1127-1136, jun. 2006, doi: 10.1109/TIE.2006.878321.

[18] C. Castillo, «Tarea 5: Control Vectorial de una Máquina».

[19] S. Li, T. A. Haskew, E. Muljadi, y C. Serrentino, «Characteristic Study of Vector-controlled Direct-driven Permanent Magnet Synchronous Generator in Wind Power Generation», *Electr. Power Compon. Syst.*, vol. 37, n.º 10, pp. 1162-1179, sep. 2009, doi: 10.1080/15325000902954052.

[20] S. Molina-Gordillo, M. Santo-Chiluisa, J. Llanos-Proano, F. Silva-Monteros, y J. Vega-Herrera, «Comparison of DC-Link Voltage Control Architectures on Grid-Side and Machine-Side for Permanent Magnet Synchronous Generator Connected to the Grid», en *2022 IEEE Sixth Ecuador Technical Chapters Meeting (ETCM)*, Quito, Ecuador: IEEE, oct. 2022, pp. 1-7. doi: 10.1109/ETCM56276.2022.9935719.

[21] S. E. Rhaili, A. Abbou, N. E. Hichami, y S. Marhraoui, «A New Strategy Based Neural Networks MPPT Controller for Five-phase PMSG Based Variable-Speed Wind Turbine», en *2018 7th International Conference on Renewable Energy Research and Applications (ICRERA)*, Paris: IEEE, oct. 2018, pp. 1038-1043. doi: 10.1109/ICRERA.2018.8566822.

[22] H. Zhou y B. Jiao, «Application of Fuzzy PID Control Based on DSP in DC-DC Boost Circuit», en *Proceedings of the 2018 3rd International Conference on Electrical, Automation and Mechanical Engineering (EAME 2018)*, Xi'an, China: Atlantis Press, 2018. doi: 10.2991/eame-18.2018.5.

[23] J. D. Feijoo, D. J. Chanchay, J. Llanos, y D. Ortiz-Villalba, «Advanced Controllers for Level and Temperature Process Applied to Virtual Festo MPS® PA Workstation», en *2021 IEEE International Conference on Automation/XXIV Congress of the Chilean Association of Automatic Control (ICA-ACCA)*, Valparaíso, Chile: IEEE, mar. 2021, pp. 1-6. doi: 10.1109/ICAACCA51523.2021.9465269.

[24] K. Elyaalaoui, M. Ouassaid, y M. Cherkaoui, «Primary frequency control using hierarchal fuzzy logic for a wind farm based on SCIG connected to electrical network», *Sustain. Energy Grids Netw.*, vol. 16, pp. 188-195, dic. 2018, doi: 10.1016/j.segan.2018.07.008.